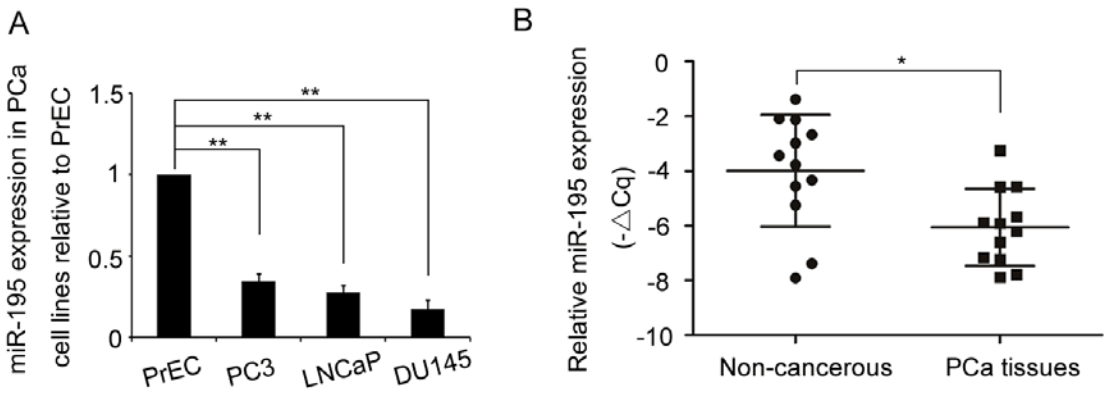

Supplementary Fig. S1. miR-195 expression is significantly reduced in both human PCa cells and tissues. (A). miR-195 levels were determined by qRT–PCR in PCa cell lines PC3, LNCaP, DU145 and non-malignant prostate epithelial cell line PrEC. miR-195 expression (miR-195/U6) of three PCa cell lines was calculated as the fold change relative to the that of PrEC cells. Data were presented as Mean ± SD. **P<0.01. (B). The relative expression of miR-195 in 12 pairs of PCa tissues and corresponding non-cancerous prostate tissues. The equation –ΔCq (−ΔCq=CqU6−CqmiR-195) was used to describe the expression level of miR-195. Data were presented as Mean ± SD. *P<0.05.

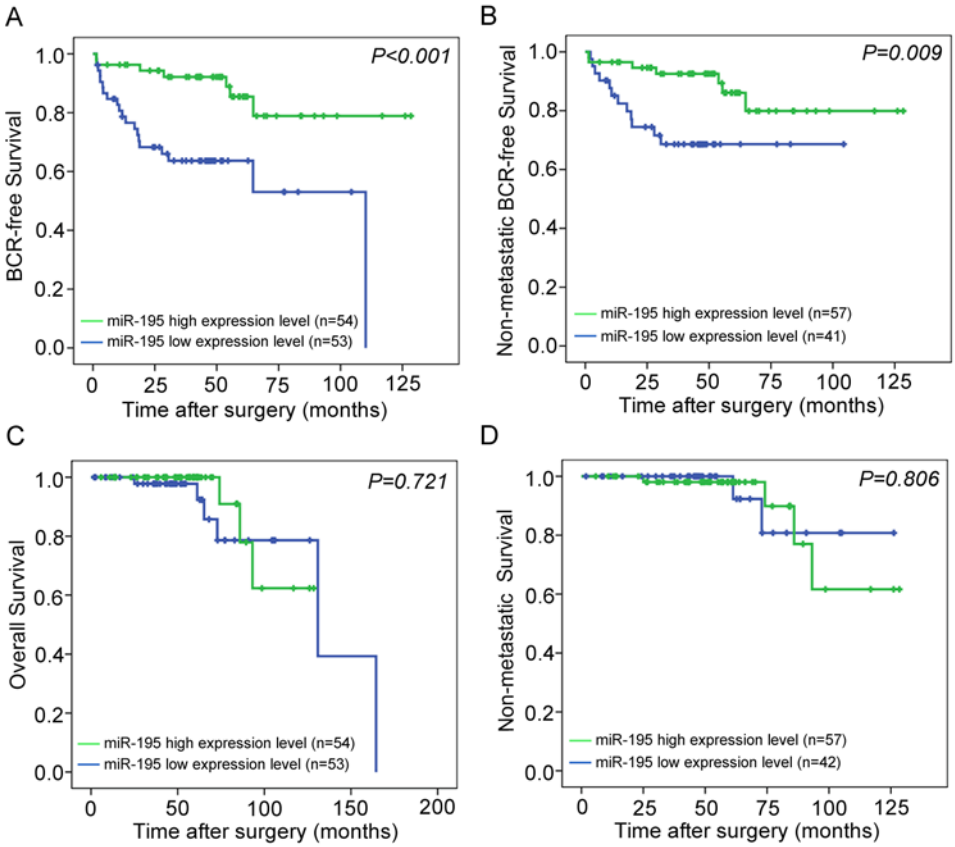

Supplementary Fig. S2. Kaplan-Meier analyses of biochemical recurrence (BCR)-free survival, non-metastatic BCR-free, survival overall survival and non-metastatic survival of prostate cancer (PCa) patients based on miR-195 expression in Taylor dataset. (A and B). miR-195 expression showed a prognostic role in BCR-free and non-metastatic BCR-free survival, as indicated by Kaplan–Meier analysis (P<0.001 and P=0.009, respectively). (C and D). miR-195 expression showed no significant difference between low and high expression groups in predicting overall and non-metastatic survival (P=0.721 and P=0.806, respectively). We dichotomized its expression level into high and low groups based on median cutoff of their expression data.

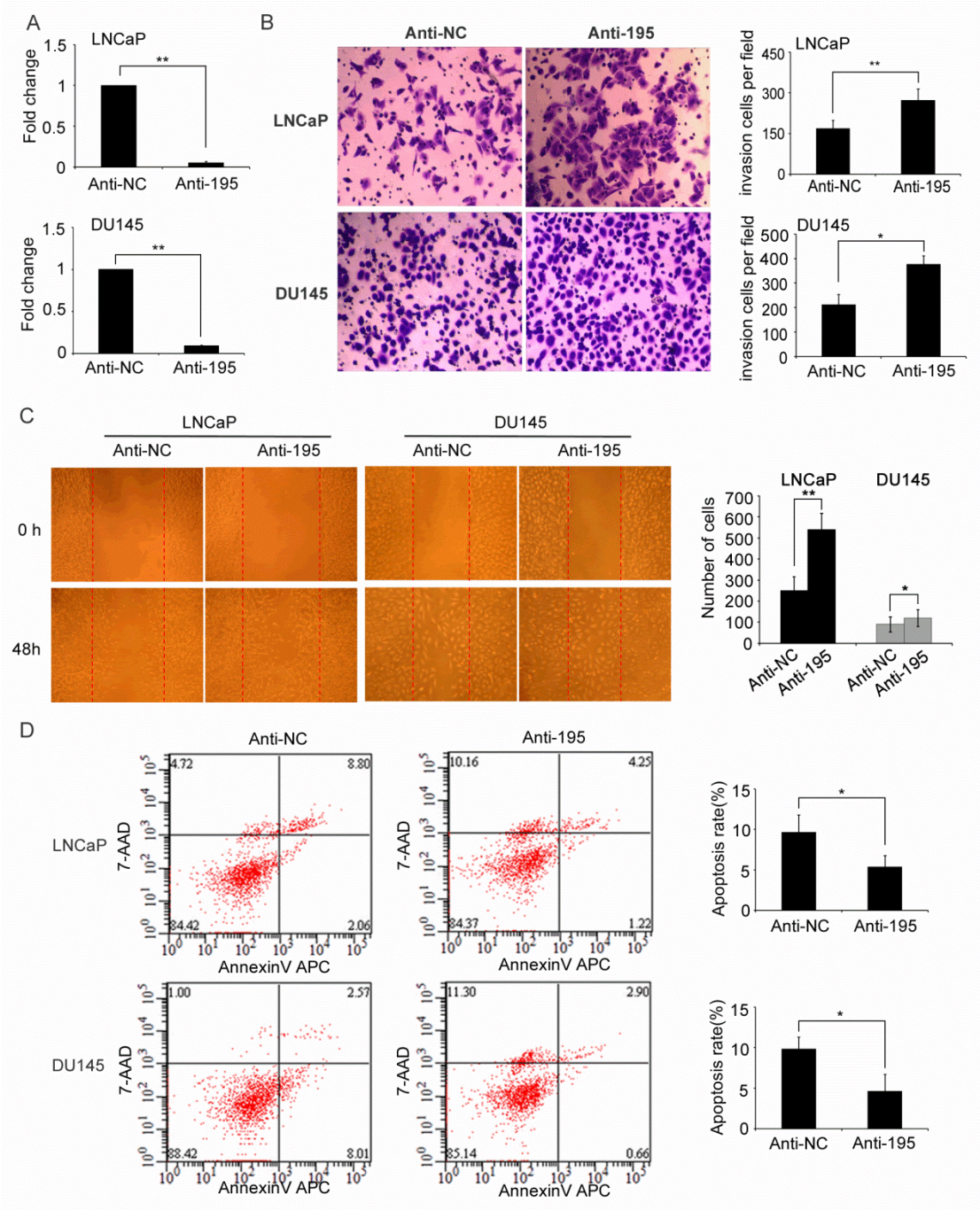

Supplementary Fig. S3. Knockdown of miR-195 expression enhances invasion, migration, but inhibits apoptosis of LNCaP and DU145 cells. (A). Lentivectors anti-195 and anti-NC were permanently transfected into LNCaP and DU145 cells. The inhibition of miR-195 in both cells was verified by qRT–PCR after transfection. miR-195 expression (miR-195/U6) was calculated as fold change relative to the NC. (B). Transwell analysis showed that miR-195 downregulation enhanced invasive

abilities of LNCaP and DU145 cells. Statistical analysis was performed with three independent experiments. (C). Wound healing assays indicated that knockdown of miR-195 expression promoted migration of LNCaP and DU145 cells. Statistical analysis was performed with three independent experiments. (D). Decreased expression of miR-195 inhibited the cell apoptosis of LNCaP and DU145 cells. Statistical analysis was performed with three independent experiments. Data were presented as Mean ± SD. *P<0.05, **P<0.01 compared with negative control.

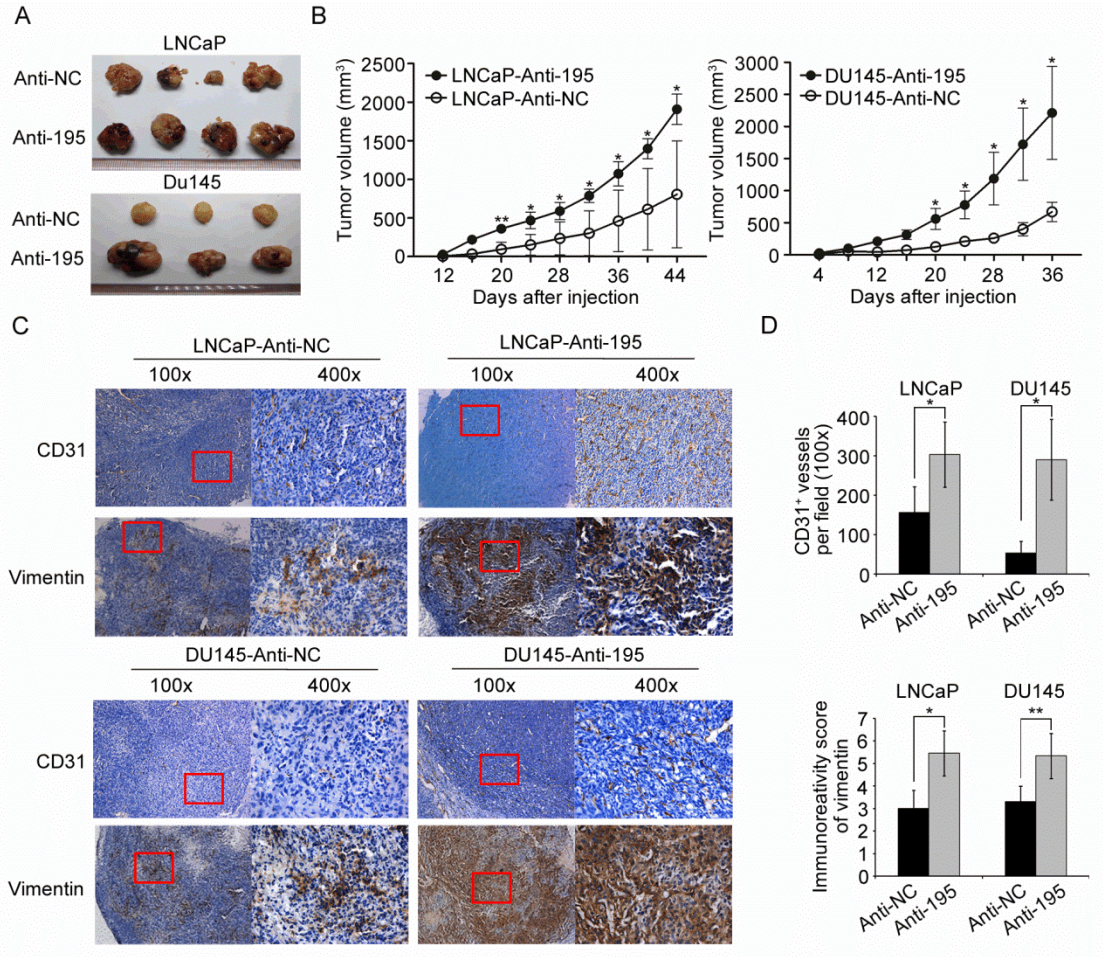

Supplementary Fig. S4. The inhibition of miR-195 enhances tumor growth, angiogenesis and invasion in vivo. (A). Lentivectors mediated inhibition of miR-195 in LNCaP and DU145 cells enhanced subcutaneous tumor growth. Tumor growth was followed for 44 days (LNCaP) or 36 days (DU145) after tumor cells injection. (B). The tumor growth curve is shown. LNCaP (n=4) and DU145 (n=3) cells with inhibited expression of miR-195 or the mock control cells were subcutaneously injected into nude mice. The tumor sizes were measured at 4-day intervals as soon as the tumors were measurable. *P<0.05 and **P<0.01 by Independent-Samples t test. Data were presented as Mean ± SD. (C). Immunochemistry analysis of the tumor xenografts. CD31 stained the cytomembrane or cytoplasm of the pan-endothelial cells of

angiogenesis. Vimentin stained the cytoplasm of the mesenchymally-derived or undergoing an EMT PCa cells (shown in the fields at a magnification of ×400). CD31 staining results indicated that the number of angiogenesis in tumor xenografts established by cells suppressed expression of miR-195 significantly increased compared with that in control tumor xenografts. Vimentin staining results indicated that the tumor xenografts established by cells suppressed expression of miR-195 expressed more Vimentin. The representative fields used for statistical analysis were presented at a magnification of ×100. (D). Vasculature density in tumor xenografts and Immunoreativity score of Vimentin, as determined by immunohistochemistry (at a magnification of ×100). The results were presented as Mean ± SD. *P<0.05, **P<0.01 compared with negative control.

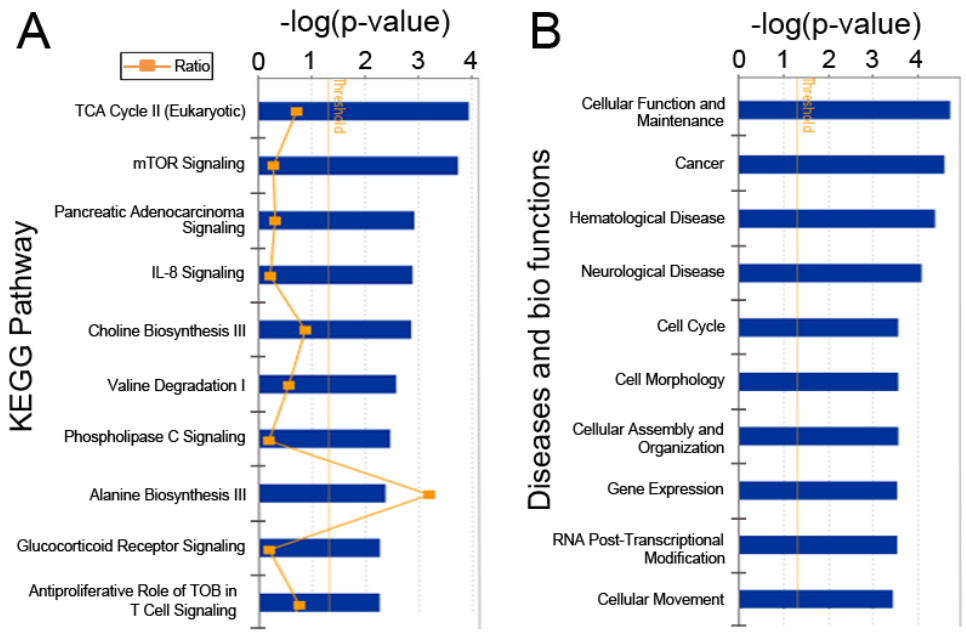

Supplementary Fig. S5. Top ten enriched KEGG pathways (A) and gene ontology (GO) biological processes (B) involved by differentially-expressed proteins induced by miR-195.

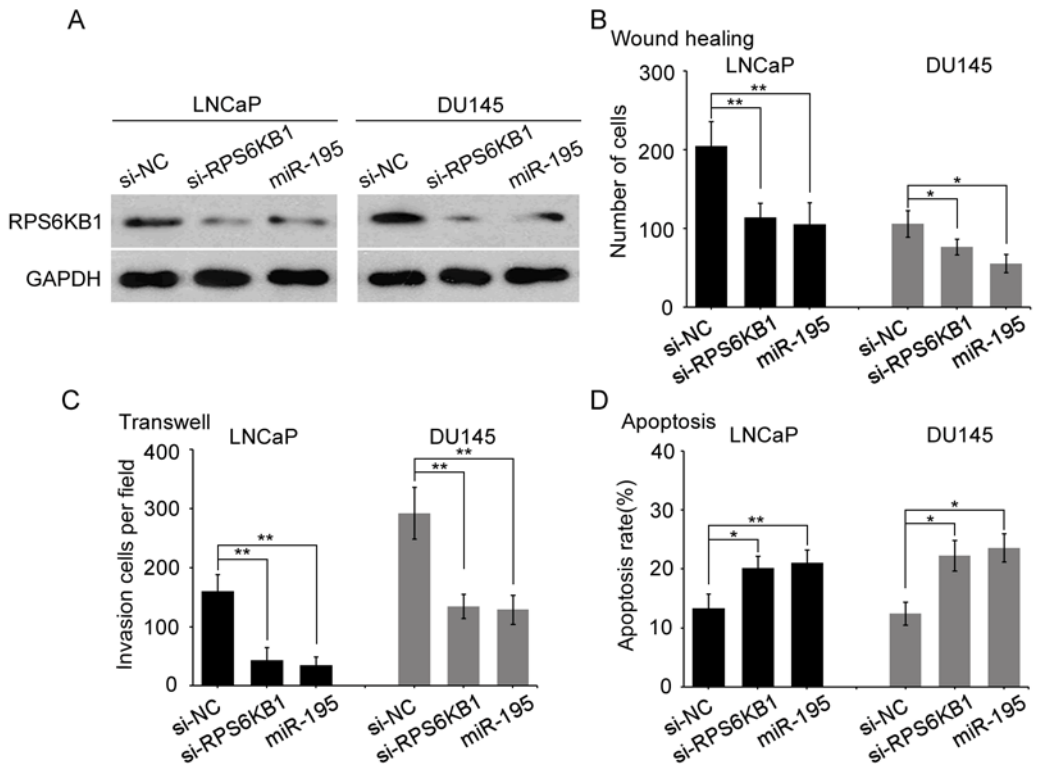

Supplementary Fig. S6. The knockdown of RPS6KB1 could imitate the tumor suppressive effects of miR-195. (A). The endogenous RPS6KB1 expression levels were detected by western blot in LNCaP and DU145 cells transfected with the miR-195 mimic or si-RPS6KB1 for 48 h. (B-D). RPS6KB1 imitated the effects associated with miR-195 overexpression in PCa cells in vitro. The in vitro effects of miR-195 and si-RPS6KB1 on cell migration, invasion and apoptosis were confirmed by wound healing, Transwell and apoptosis assays in LNCaP and DU145 cells transfected with miR-195, si-RPS6KB1 or si-NC. The data represented the Mean ± SD of three independent experiments. *P<0.05, **P<0.01 compared with control.

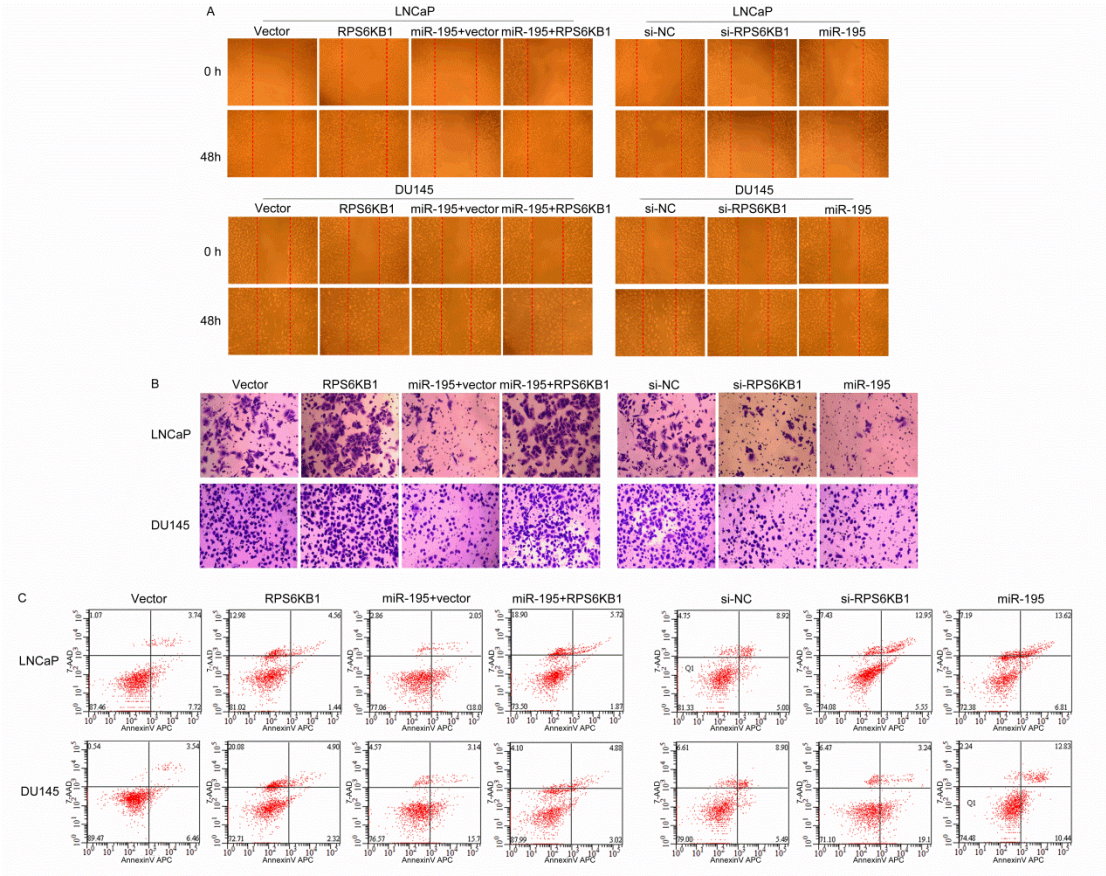

Supplementary Fig. S7. The re-expression and knockdown of RPS6KB1 could respectively rescue and imitate the tumor suppressive effects of miR-195. The wound-healing (A), Transwell invasion (B) and apoptosis (C) assays in LNCaP and DU145 cells were performed after the treatment of Oligonucleotides and/or plasmids for 48h.

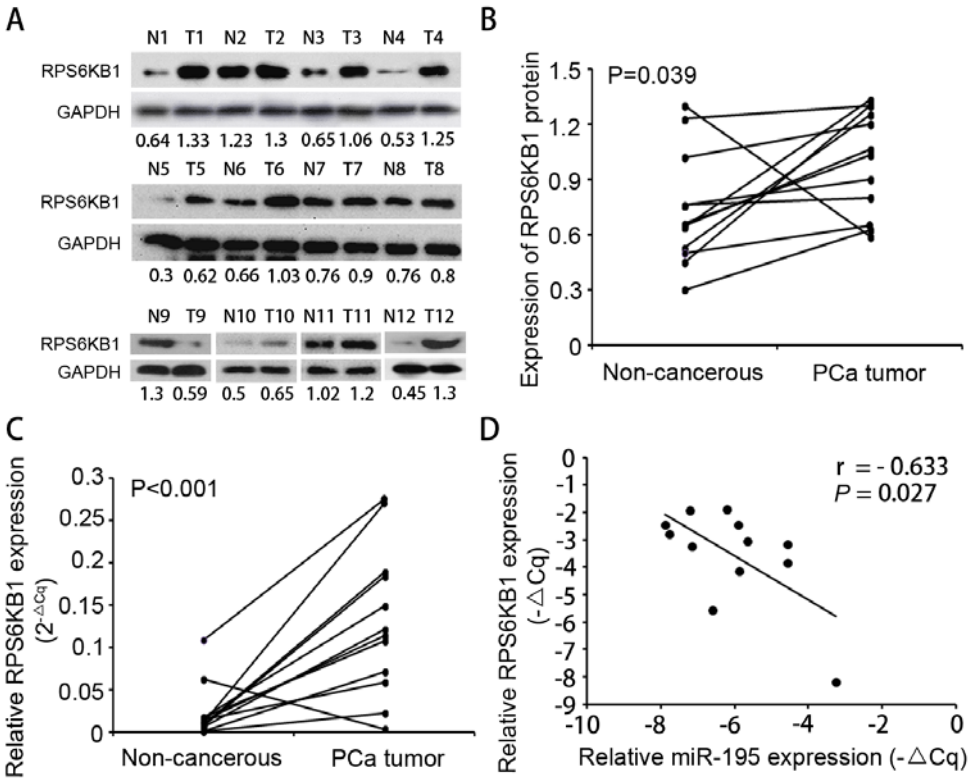

Supplementary Fig. S8. Reverse correlation between miR-195 and RPS6KB1 expression in human PCa tissues. (A-B). Expression of RPS6KB1 in 12 pairs of PCa and the corresponding adjacent nontumourous tissues was determined by western blot. The results indicated that RPS6KB1 expression in PCa tissues were higher than that in adjacent non-cancerous prostate tissues (P=0.039). (C). qRT-PCR analysis revealed that RPS6KB1 mRNA expression was significantly up-regulated in 12 PCa tissues (P<0.001). The data were presented as Mean ± SD. (D). The Spearman Correlation analysis clearly suggested an inverse relationship between RPS6KB1 mRNA and miR-195 expression in PCa tissues (r=-0.633, P=0.027).

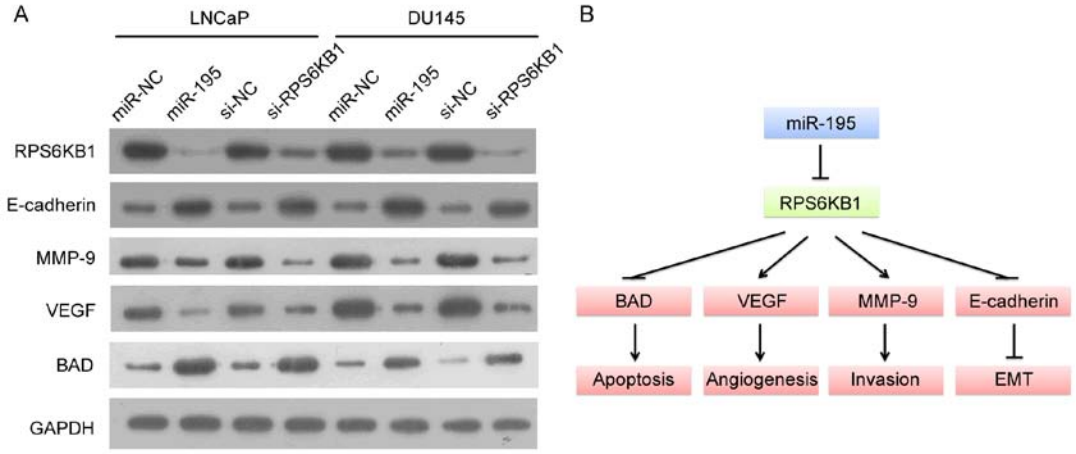

Supplementary Fig. S9. MMP-9, VEGF, BAD and E-cadherin function as downstream effectors of miR-195-RPS6KB1 axis. (A). Western blot analysis was performed to detect the expression levels of MMP-9, VEGF, BAD and E-cadherin proteins levels in LNCaP and DU145 cells transfected with miR-195 mimics, miR-NC, si-RPS6KB1 or si-NC for 48h. (B). Schematic diagram of miR-195-RPS6KB1/MMP-9/VEGF/BAD/E-cadherin signaling.